Self-organized criticality and directed percolation

1999 J. Phys. A: Math. Gen. 32 2633

(http://iopscience.iop.org/0305-4470/32/14/004)

J. Phys. A: Math. Gen. **32** (1999) 2633–2644. Printed in the UK PII: S0305-4470(99)99081-9

Self-organized criticality and directed percolation

Alexei Vázquez† and Oscar Sotolongo Costa†‡

† Department of Theoretical Physics, Faculty of Physics, The University of Havana, Havana 10400, Cuba

‡ Departamento de Fisica-Matematica y Fluidos, Facultad de Ciencias, UNED, Senda del Rey S/N, Apdo. 60141, Madrid 28080, Spain

Received 5 November 1998

Abstract. A sandpile model with a stochastic toppling rule is studied. The control parameters and the phase diagram are determined through a mean-field approach, and the subcritical and critical regions are analysed. The model is found to have some similarities with directed percolation, but the existence of different boundary conditions and conservation law leads to a different universality class, where the critical state is extended to a line segment due to self-organization. These results are supported by numerical simulations in one dimension. This model constitutes a simple model which captures the essential difference between ordinary nonequilibrium critical phenomena, like directed percolation, and self-organized criticality.

1. introduction

The idea of self-organized criticality (SOC) was introduced to describe the behaviour of a class of extended dissipative dynamical systems which naturally evolve to a critical state, consisting of avalanches propagating throughout the system [1]. From the very beginning it was observed that this new idea has some connections with ordinary critical phenomena [2]. More recently a novel mean-field (MF) analysis of SOC was presented, which pointed out similarities between SOC models and models with absorbing states [3]. Directed percolation (DP) [4] is one of the simplest and most recurrent models with absorbing states. Under very general guidelines (locality, scalar variable, etc) it has been proposed that a wide range of models would fall into the DP universality class [4–6]. Although SOC models do not belong to the DP universality class they do have some connection with DP [7–9]. Indeed, Maslov and Zhang [10], have argued that for space dimensionality $d \geqslant 2$, a version of a stochastic sandpile model is related to $(d + 1)$-dimensional directed percolation with time interpreted as the preferred direction.

Recently, Tadić and Dhar have shown that a kind of stochastic sandpile model has some analogies with DP [9]. They studied a directed sandpile model in which unstable sites topple with probability p. They observed that above a critical threshold p_c the system shows SOC, while below the threshold the system is not critical. The critical probability was identified with the threshold for DP in a square lattice and the scaling exponents were obtained in terms of DP exponents. However, they could not give a detailed description of the phase diagram, since their analysis was limited to the SOC regime above p_c, while the state below p_c could not be characterized.

Following the work of Tadić and Dhar, we study a class of stochastic sandpile models with an undirected toppling rule. As in their model, sites topples with a probability p but now grains are distributed to each nearest neighbour. In order to provide a theoretical description

0305-4470/99/142633+12$19.50

of the model, we have generalized the MF theory by Vespignani and Zapperi [3] including the control parameter p. In this way we obtain the complete phase diagram of the model. The existence of a critical probability p_c and a quasi-stationary state below p_c are obtained. Based on MF analysis and on the evolution rules we argue that the state below p_c is similar to DP, but with different boundary conditions. Using this hypothesis we apply the scaling theory developed for DP to the present stochastic sandpile model. Numerical simulations in one dimension support our hypothesis.

The paper is organized as follows. In section 2 we introduce the dynamical evolution rules for the stochastic version of the Bak–Tang–Wiesenfeld (BTW) model. We perform a single-site MF approximation and determine the average densities in the stationary state. It is found that the driving rate h and p are the only control parameters and that the system is critical in the line segment ($h = 0^+$, $p_c \leqslant p \leqslant 1$). Then, in section 3 we show the connection with DP and derive some scaling relations. In order to check our predictions we have performed numerical simulations in one dimension, and the main results are presented in section 4. Finally, the summary and conclusions are given in section 5.

2. MF theory

We establish our stochastic sandpile model defined as follows. An integer variable z_i (height or energy) is assigned to each site of a d-dimensional lattice and energy is added to the system at a rate h. When a site receives a grain and its energy exceeds a threshold z_c then, with probability p, it relaxes according to the following rules $z_i \to z_i - g$ and $z_j \to z_j + 1$ at each of g nearest neighbours. Open boundary conditions are assumed. One may call this model a non-Abelian sandpile model with stochastic rules. The non-Abelian behaviour makes it different from other stochastic models such as the Manna model [11]. However, we will simply call it the stochastic sandpile model.

The first step towards a comprehensive understanding of critical phenomena is provided by MF theory, which gives insight into the fundamental physical mechanism of the problem. Thus, we start analysing the stochastic sandpile model through a MF approach. With this simple picture we introduce the connection with directed percolation.

The first MF theory for sandpile models was introduced by Tang and Bak [2], and only deterministic toppling rules were considered. Later on, Caldarelli [12] generalized this MF theory to sandpile models with a certain degree of stochasticity in the toppling rules. Particularly, Caldarelli studied sandpile models where p is a function of z_i, such that $0 < p(z) < 1$ below the critical threshold z_c and $p(z) = 1$ above. Their MF theory and further numerical simulations reveal that the stochastic rules, introduced in this way, change the average of z, but do not destroy the critical state [12]. In the sandpile models analysed by Caldarelli p is not a control parameter, its average value is determined by the system dynamics. In these models the system self-organizes to a stationary sate, where $\langle p(z) \rangle$ is such that the system remains in a critical state. In contrast, in the stochastic sandpile model considered here p is a control parameter. It is expected that for sufficiently small values of p the critical state will be destroyed. Therefore, we have to develop a MF theory where p appears explicitly as a control parameter.

Recently, Vespignani and Zapperi [3] have introduced a more general framework. In contrast to previous theories, their MF approach is not based on some particular sandpile model but on general considerations which are common to all of them, which are even extendable to other SOC models [3]. Within this formalism, SOC appears as a special case of nonequilibrium critical phenomena. They classify the states for each site into three categories: stable (s), critical (c), and active (a). Stable sites are those that cannot become active by the addition

of energy, critical sites are those that become active by the addition of energy and active sites are relaxing and transfer energy to their neighbours. These definitions become very clear in a deterministic sandpile model. For instance (assuming the probability that a site receives two energy grains simultaneously is negligible) sites with $z < z_c - 1$ are stable, those with $z = z_c - 1$ are critical and those with $z > z_c$ are active. However, in the stochastic model sites with $z \geqslant z_c$ topple with probability p. Again sites with $z < z_c - 1$ are stable since they can never become active after receiving a single energy grain. Nevertheless, those with $z \geqslant z_c - 1$ do not have a well-defined state. For instance, sites with $z = z_c - 1$ may topple after receiving one energy grain and, therefore, they cannot be stable. However, they are not strictly critical because only a fraction p of them will topple after receiving a grain of energy. Hence, in the case of stochastic sandpile models the subdivision in stable, critical and active does not cover all the possible states each site can assume, i.e. $\rho_s + \rho_c + \rho_a < 1$.

Let us divide the states that each site can assume in stable (s), unstable (u), and active (a) and denote their average densities by ρ_s, ρ_u and ρ_a, respectively. The definitions of stable and active sites are the same as considered by Vespignani and Zapperi, while unstable sites are now those sites that *may* become active by the addition of energy. Under these definitions, sites with $z < z_c - 1$ are stable, those with $z = z_c - 1$ are unstable and those with $z \geqslant z_c$ may be either unstable or active. Only a fraction p of the unstable sites will become active after receiving energy and, therefore, are critical sites, i.e.

$$\rho_c = p\rho_u. \tag{1}$$

This equality makes the connection between our MF approach and that of Vespignani and Zapperi [3]. In the deterministic limit $p = 1$ there is no difference between critical and unstable sites.

To study the dynamics of the stochastic sandpile model we consider the following Markov process for the average densities

$$\frac{\partial}{\partial t}\rho_n = \sum_{m \neq n} T_{mn}\rho_m - \sum_{m \neq n} T_{nm}\rho_n \tag{2}$$

where T_{nm} are the transition rates from state n to state m (see figure 1). By constructing the model in one time step stable sites never becomes active and unstable sites never become stable, i.e. $T_{sa} = T_{us} = 0$. $T_{as} = q$ and $T_{au} = 1 - q$, where q is the fraction of active sites that becomes stable after relaxing. In deterministic models q should be taken as equal to one [3]. However, in stochastic models z may take large enough values compared with z_c in such a way that an active site may become unstable after relaxing, i.e. $q < 1$. Although an active site with $z \gg z_c$ may remain active due to an addition of energy this type of transition is of second order, and can be neglected for small ρ_a and h. The transition rates T_{su} and T_{ua} depend on the

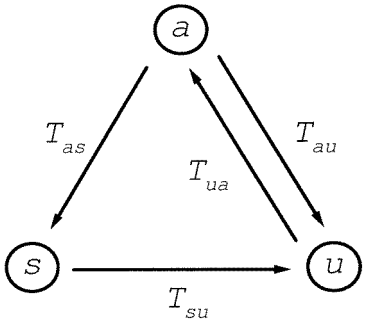

Figure 1. Schematic representation of the single site approximation for the stochastic sandpile model. Sites are divided in stable (s) unstable (u) and active (s). T_{mn} are the transition rates for the state m to n. Transitions which do not take place are not represented.

probability per unit time that a site receives energy. If ρ_a and h are small then the probability per unit time that a site receives more than one grain of energy is negligible, and the probability per unit time that a site receives a grain of energy may be approximated by

$$h_1 = h + (g - \epsilon)\rho_a \tag{3}$$

where $g - \epsilon$ is the effective number of nearest neighbours and ϵ is the dissipation rate per toppling event, an effective parameter which accounts for boundary dissipation. If u (p) is the fraction of stable (unstable) sites that become unstable (active) after receiving a grain of energy then $T_{su} = uh_1$ ($T_{ua} = ph_1$). Taking into account these considerations the system of differential equation (2) reduces to

$$\frac{\partial}{\partial t}\rho_a = -[1 - (g - \epsilon)\rho_c]\rho_a + \rho_c h + \mathrm{O}(h^2, h\rho_a) \tag{4}$$

$$\frac{\partial}{\partial t}\rho_s = q\rho_a - u(h + g\rho_a)\rho_s + \mathrm{O}(h^2, h\rho_a) \tag{5}$$

together with the normalization condition

$$\rho_s + \rho_u + \rho_a = 1. \tag{6}$$

Notice that, among unstable sites, only the fraction of critical sites $\rho_c = p\rho_u$ contributes to the system dynamics, the other fraction is only relevant through the normalization condition in equation (6). The system of equations is completed by the equation of energy balance:

$$\frac{\partial}{\partial t}E = (h - \epsilon\rho_a)L^d \tag{7}$$

where E is the total energy of the system, hL^d is the average influx of energy and $\epsilon\rho_a L^d$ the average outflux of energy.

2.1. Critical state

In the stationary state ($\frac{\partial \rho_n}{\partial t} = 0$, $\frac{\partial E}{\partial t} = 0$) from equations (4)–(7) and equation (1), we obtain

$$\rho_a = \frac{h}{\epsilon} \qquad \rho_c = \frac{1}{g} + \mathrm{O}(h) \tag{8}$$

$$\rho_u = \frac{1}{pg} + \mathrm{O}(h) \qquad \rho_s = \frac{pg - 1}{pg} + \mathrm{O}(h) \tag{9}$$

$$\frac{q}{u} = \frac{pg - 1}{p} + \mathrm{O}(h). \tag{10}$$

Comparing these expressions with the ones obtained by Vespignani and Zapperi [3], we observe that the average densities of active and critical sites have the same stationary solutions. The differences appear in the density of stable and unstable sites, which now depend on the new control parameter p.

For $1/g \leqslant p \leqslant 1$ we have $1/g \leqslant \rho_u \leqslant 1$, $0 \leqslant \rho_s \leqslant (g - 1)/g$ and, therefore, there is no inconsistency in the stationary solutions obtained above. In this range of p, within the MF approach, there is no distinction between the critical state of stochastic and deterministic sandpile models. The model is critical in the double limit $h, \epsilon \to 0$ and $h/\epsilon \to 0$ [3] and the susceptibility,

$$\chi = \frac{\partial \rho_a}{\partial h} = \frac{1}{\epsilon} \tag{11}$$

diverges at the critical state. For a small perturbation around the subcritical state $\rho_a = h/\epsilon + \Delta\rho_a$, $\rho_c \approx 1/g$ and from equation (4) one obtains

$$\Delta\rho_a(t) \propto \exp(-\epsilon t/g) \tag{12}$$

in agreement with the result for deterministic models [3].

From equations (11) and (12) one may think that ϵ is a control parameter of the model. However, if the dissipation takes place only at the boundary then ϵ will decrease with increasing system size, because the number of active sites in the bulk grows faster than the number of active sites at the boundary. Hence, we are just dealing with a finite-size effect. The statement that the system is not in a critical state is equivalent to the statement that there is no critical state in a finite system. If dissipation takes place only at the boundary ϵ is not a control parameter, it just reflects a finite-size effect which at the same time is a necessary condition to obtain a stationary state. In this sense, the criticality here is different from the criticality at phase transitions where boundary effects always disappear in the thermodynamic limit [1].

In contrast, the driving field h is actually a control parameter. Since h must satisfy $h < \epsilon$ and $\epsilon \to 0$ when $L \to \infty$, then we must fine tune h to zero in order to obtain criticality in the thermodynamic limit. The timescale separation becomes a necessary condition for criticality. Now if we assume separation of timescales then p will be the only control parameter of the model. This hypothesis is fulfilled in the computer simulations, where a new grain of energy is added only once there are no active sites in the lattice.

2.2. Breakdown of SOC by stochastic rules

When $0 < p < 1/g$ the stationary solutions in equations (8)–(10) are no longer valid because they imply $\rho_u > 1$ and $\rho_s < 0$. Let us analyse the variation of ρ_u and ρ_c with p to understand the origin of this inconsistency. In the deterministic case $p = 1$, there is no distinction between unstable and critical sites, i.e. $\rho_c = \rho_u = 1/g$. However, when $p < 1$ critical sites are a fraction of unstable sites $\rho_c = p\rho_u$. Hence, since in the stationary state $\rho_c = 1/g$, the system has to self-organize increasing the average density of unstable sites up to $\rho_u = 1/pg > 1/g$ and decreasing the average density of stable sites. But when $p = 1/g$ we have $\rho_u = 1$ and $\rho_s = 0$. Therefore, when p keeps decreasing the system cannot provide more unstable sites. Then $\rho_c < 1/g$ and the stationary solutions in equations (8)–(10) fall down.

Let us assume that for $0 < p < 1/g$ the average densities reach an stationary state, which of course cannot be given by equations (8)–(10). From equation (4) it results in

$$\rho_a = \frac{\rho_c h}{1 - (g - \epsilon)\rho_c}. \tag{13}$$

Using this expression in equation (7), one obtains

$$\frac{\partial}{\partial t} E = \frac{1 - g\rho_c}{1 - (g - \epsilon)\rho_c} h L^d. \tag{14}$$

According to equation (1), $\rho_c = p\rho_u \leqslant p < 1/g$, independently of ρ_u. Hence, $\frac{\partial E}{\partial t} > 0$ and the total energy will increase with time. Moreover, stable sites are those with $z < z_c - 1$ and, therefore, it is expected that after a long enough time there will be no stable sites remaining. In this quasi-stationary state, the energy increases with time and the average densities will take the stationary values

$$\rho_a = \frac{hp}{1 - (g - \epsilon)p} \qquad \rho_c = p + \mathrm{O}(h) \tag{15}$$

$$\rho_u = 1 + \mathrm{O}(h) \qquad \rho_s = 0 \tag{16}$$

$$q = 0. \tag{17}$$

Now it is clear that p is a control parameter for the class of stochastic sandpile models analysed here.

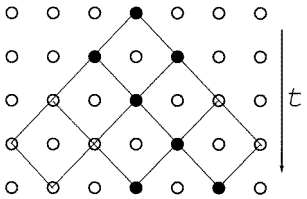

Figure 2. Evolution of an avalanche in the stochastic sandpile model. Empty sites are inactive (stable + unstable) and filled sites are active. This figure clearly shows that the avalanche evolves in a directed square lattice, where the probability that a site is present is ρ_c.

The susceptibility in this region is given by, assuming $\epsilon \ll g$,

$$\chi = \frac{p}{1 - pg}. \tag{18}$$

For a small perturbation around the subcritical state, we have $\rho_a = \chi h + \Delta\rho_a$, and $\rho_c \approx p$. Then from equation (4) one obtains, again considering $\epsilon \ll g$,

$$\Delta\rho_a(t) \propto \exp[-(1 - pg)t]. \tag{19}$$

The critical state breaks down by the stochastic rules, once $p < p_c$. To reach the critical state we have to fine-tune p. Near the critical threshold $1/g$ both the susceptibility $\chi \sim (p_c - p)^{-1}$ and the characteristic time $\sim (p_c - p)^{-1}$ diverge.

In summary, we have found a critical probability p_c above which the system is in a SOC state, while it is in a subcritical state below that value.

3. Scaling theory

ρ_c is the probability that a site becomes active after receiving a grain of energy. In the absence of an external field, it is also the probability that a site becomes active if one of its neighbours was active in the previous step. This problem is equivalent to site-directed percolation in $d + 1$ dimensions (d spatial dimensions + time), ρ_c being the probability that a site is present. The only difference remains in the boundary conditions: while in DP the system is assumed to be of infinite extent, here we deal with a finite system with open boundaries. This picture is better represented in figure 2.

3.1. The case $0 < p < p_c$

According to MF theory, below p_c there are no stable sites and the fraction of critical sites is given by $\rho_c = p$. Thus, the evolution rules correspond to DP. The existence of different boundary conditions may lead to differences in some scaling exponents. However, the nature of the phenomena is the same. For instance, DP near a wall reveals that the correlation length exponents are identical to those obtained in DP in an infinite lattice [13], but other exponents take different values. This is a consequence of the fact that in DP near a wall the avalanches are a subset of the avalanches in DP in an infinite lattice. We thus expect a similar behaviour in the stochastic sandpile model below p_c. In this case, avalanches starting far from the boundary behave as in DP in an infinite lattice, while avalanches starting near the boundary behave like the avalanches in DP near a wall. Hence, the correlation lengths and the correlation length exponents are identical to those for DP in an infinite lattice, i.e.

$$\xi_\perp \sim (p_c - p)^{-\nu_\perp} \qquad \xi_{||} \sim (p_c - p)^{-\nu_{||}} \tag{20}$$

where $\xi_\perp$ and $\xi_{||}$ are the spatial and temporal correlation lengths, respectively, and $\nu_\perp$ and $\nu_{||}$ the correlation length exponents.

On the other hand, based on this analogy with DP, we write the following scaling relation for the average density of active sites at site x and time t, given a site active in the origin $x = 0$ at $t = 0$,

$$\rho_a(x,t) = t^{\eta-\frac{2}{z}} f\left(\frac{x^2}{t^{2/z}}, \frac{t}{\xi_{||}}\right) \tag{21}$$

first introduced by Grassberger and de la Torre [14] in the context of DP. Here η is a scaling exponent and z the dynamic scaling exponent, as usually defined in the context of critical phenomena. Moreover, the probability that the avalanche survives up to time t is given by

$$P(t) = t^{-\delta} g\left(\frac{t}{\xi_{||}}\right) \tag{22}$$

where δ is another scaling exponent. From equation (21) one can derive the scaling laws for the average number of active sites $n(t)$, the cluster mass $m(t)$ and the mean-squared displacement $R^2(t)$ at time t, resulting in

$$\begin{aligned} n(t) &= \int \mathrm{d}^d x\, \rho_a(x,t) = t^{\eta} f_1\left(\frac{t}{\xi_{||}}\right) \\ m(t) &= \int_0^t \mathrm{d}t'\, n(t') = t^{1+\eta} f_2\left(\frac{t}{\xi_{||}}\right) \\ R^2(t) &= \frac{1}{n(t)} \int \mathrm{d}^d x\, \rho_a(x,t) x^2 = t^{2/z} f_3\left(\frac{t}{\xi_{||}}\right). \end{aligned} \tag{23}$$

The exponent z is not independent, since $t \sim r^z$. From equation (20) one obtains

$$z = \frac{\nu_{||}}{\nu_\perp} \tag{24}$$

and it is therefore identical to that for DP in an infinite lattice. Nevertheless, the exponents η and δ depend on the boundary conditions, as is observed in DP near a wall [13].

3.2. The case $p_c \leqslant p < 1$

We assume that the scaling laws in equations (21)–(23) are also valid above p_c, but with $\xi_{||} = \xi_{||}(L)$. In this region the dynamical evolution is independent of p and the characteristics length and time depend only on the lattice size L, according to

$$\xi_\perp \sim L \qquad \xi_{||} \sim L^z. \tag{25}$$

However, as is shown below, for $p > p_c$ the global conservation introduces a constraint between the exponents η and z.

Let us calculate the average energy flux $J(r)$ outside an sphere of radius r, given a grain of energy added at the origin $r = 0$ at $t = 0$. The energy flux is proportional to the gradient of the average density of active sites and, therefore,

$$J(r) \propto r^2 \int \mathrm{d}t\, \frac{\partial}{\partial r} \rho_a(r,t). \tag{26}$$

Substituting the scaling relation for $\rho_a(r,t)$ (21) in this expression results in

$$J(r) = r^{(1+\eta)z-2} f_4\left(\frac{r}{\xi_\perp}\right). \tag{27}$$

Now, conservation implies that $J(r) = 1$ for $r < \xi_\perp \sim L$ and, therefore,

$$(1+\eta)z = 2. \tag{28}$$

This scaling relation may seem unusual: a more familiar expression is obtained from the mean avalanche size

$$\langle s \rangle = \int \mathrm{d}t\, n(t) \sim L^{(1+\eta)z} = L^2. \tag{29}$$

This scaling relation was previously obtained by Dhar [16] but for a particular sandpile model. Here we have demonstrated, using scaling arguments, that it holds for any sandpile model with global conservation.

3.3. Directed models

In the directed stochastic model there is a preferential direction l for the avalanche evolution. Taking this preferential direction as the equivalent of time in undirected models we can apply the scaling theory developed above to directed models. This means that the scaling relations in equations (21)–(23) are also valid for directed models, but now x is a $(d-1)$-dimensional vector in the space of the nonpreferential directions and t gives the evolution in the direction l.

Another important difference between undirected and directed models is the place where toppling takes place during the evolution of the avalanche. In the undirected model not only the sites in the avalanche front, but also sites inside this front may be active, transfering energy to their neighbours. In contrast, in directed models all active sites are in the avalanche front, i.e. at step t all active sites are in the layer $l = t$. Moreover, active sites in layer l transfer energy only to those neighbours in layer $l + 1$. Hence, in directed models the energy flux follows the preferential direction, while in the undirected case the energy flows in all directions.

An immediate consequence of this difference is that in directed models the average outflux of energy from the $l = t$ to the $l + 1$ layer, which is proportional to the average number of active sites in the $l = t$ layer, equals one and, therefore,

$$n(t) \sim 1. \tag{30}$$

Then, from equation (23) one obtains

$$\eta = 0. \tag{31}$$

Thus the energy balance leads to a different constraint for the set of scaling exponents (η, z, δ), i.e. the directed model belongs to a different universality class.

4. Numerical simulations and discussion

In order to test our predictions, we have performed some numerical simulations for the stochastic sandpile model in one dimension. We have investigated both regimes of the phase diagram, the region similar to DP below p_c and the SOC region above. In both regions we start with a flat pile, i.e. zero height in all sites, and let the system evolve to the stationary state. Above p_c the stationary state is characterized by a constant average energy per site, which was taken as the stationary condition. Below p_c the energy increases with time and, therefore, we look for another stationarity criterion. According to MF theory in the quasi-stationary state below p_c we have $\rho_u = 1$, which was taken as the stationary condition. In all cases we start measuring after the system reaches the stationary state. Averages were taken over 10 000 000 avalanches below p_c and over 1000 000 avalanches above. Below p_c we use the lattice size $L = 10\,240$, which was large enough to avoid finite-size effects for the values of p considered. Above p_c we use $p = 0.708$ and different lattice sizes.

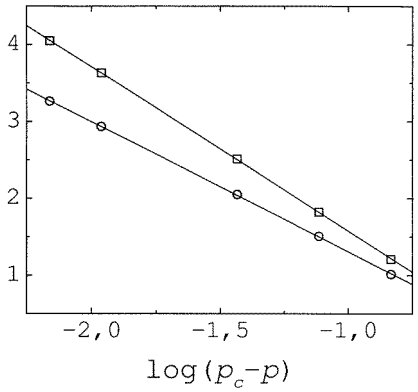

Figure 3. The correlation lengths $\log \xi_\perp$ (squares) and $\log \xi_{||}$ (circles) as a function of p in the subcritical state. The lines are linear fits to the log–log plot.

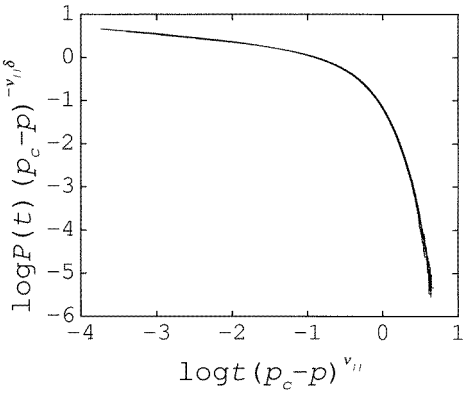

Figure 4. Data collapse plot for $P(t)$ in the subcritical state for $p = 0.670$, 0.688, 0.696 and 0.700.

To obtain an estimate of p_c we have calculated the correlation lengths in the subcritical state for different values of p and fitted the numerical data to the scaling laws in equation (20). These magnitudes were computed in the simulations using the following expressions

$$\begin{aligned} \xi_\perp^2 &\sim \frac{\sum_{t=0}^{\infty}\sum_{i=0}^{L}(i-i_0)^2\rho_{ai}}{\sum_{t=0}^{\infty}\sum_{i=0}^{L}\rho_{ai}} \\ \xi_{||} &\sim \frac{\sum_{t=0}^{\infty}\sum_{i=0}^{L}t\rho_{ai}}{\sum_{t=0}^{\infty}\sum_{i=0}^{L}\rho_{ai}} \end{aligned} \tag{32}$$

where i_0 is the position of the initial active site, t is the number of steps measured in the timescale of the avalanche and $\rho_{ai} = 1$ ($\rho_{ai} = 0$) in active (unstable) sites.

The log–log plot of the correlation lengths versus $p_c - p$ is shown in figure 3. The best fit to the numerical data was obtained for

$$\begin{aligned} &p_c = 0.707 \pm 0.002 \qquad (0.705\,485) \\ &\nu_\perp = 1.07 \pm 0.03 \qquad (1.0968) \\ &\nu_{||} = 1.71 \pm 0.03 \qquad (1.7338). \end{aligned} \tag{33}$$

Enclosed in parenthesis are the series expansion estimates for DP in an infinite lattice reported in [15]. Within the numerical error there is a complete agreement between the values reported here and those of DP.

Then, we proceed to determine the exponents δ, η and z from the data collapse plots of $P(t)$, $m(t)$ and $R^2(t)$, using the scaling laws in equation (23). The corresponding plots are shown in figures 4–6. The best data collapse were obtained for

$$\begin{aligned} &\delta = 0.18 \pm 0.01 \qquad (0.159\,47) \\ &\eta = 0.27 \pm 0.01 \qquad (0.313\,68) \\ &z = 1.59 \pm 0.01 \qquad (1.580\,74) \\ &\nu_{||} = 1.73 \pm 0.01 \qquad (1.7338) \\ &(1+\eta)z = 2.02 \pm 0.02. \end{aligned} \tag{34}$$

From the data collapse we have obtained a better estimate for $\nu_{||}$ and, using the scaling relation (24) and the value of z in (34), we obtain the best estimate for $\nu_\perp$:

$$\nu_\perp = 1.09 \pm 0.02 \qquad (1.0968). \tag{35}$$

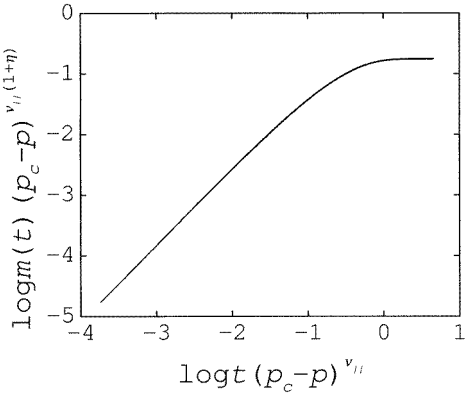

Figure 5. Data collapse plot for $m(t)$ in the subcritical state for $p = 0.670$, 0.688, 0.696 and 0.700.

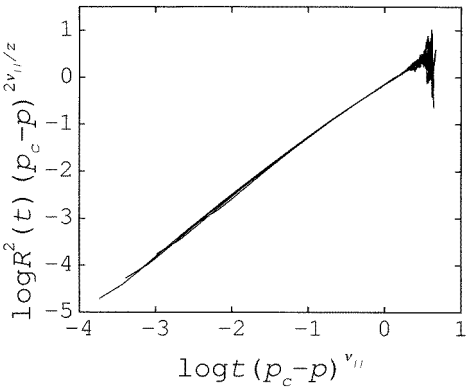

Figure 6. Data collapse plot for $R^2(t)$ in the subcritical state for $p = 0.670$, 0.688, 0.696 and 0.700.

As was expected the critical probability, the correlation length exponents, and z are identical, within the numerical error, to those reported for DP in an infinite lattice, while the η and δ results are different.

Now let us analyse the numerical simulations in the SOC region $p_c \leqslant p < 1$. In this case we can estimate the critical probability from the divergence of the average energy per site $\langle E\rangle$ near p_c. In the SOC region $\langle E\rangle$ reaches a stationary value but increases with time below p_c. Therefore $\langle E\rangle$ must diverge when the system approaches the critical probability from above. We observe that the divergence of $\langle E\rangle$ can be fitted to the power-law dependence $\langle E\rangle \sim (p - p_c)^{-\lambda}$, where λ is a scaling exponent. In figure 7 we have plotted the best fit to the numerical data for a lattice size $L = 1280$, resulting in

$$p_c = 0.704 \pm 0.01 \qquad (0.705\,485) \tag{36}$$

which is close to the DP value.

Then we proceed to determine the exponents δ, η and z from the data collapse above p_c, using the scaling laws in equations (23) and (25). The best data collapse are shown in figures 8–10 with

$$\begin{aligned} &\delta = 0.18 \pm 0.01 \qquad (0.159\,47)\\ &\eta = 0.28 \pm 0.01 \qquad (0.313\,68)\\ &z = 1.57 \pm 0.01 \qquad (1.580\,74)\\ &(1+\eta)z = 2.01 \pm 0.02. \end{aligned} \tag{37}$$

From the comparison of these values with those in equation (34) we conclude that the scaling exponents δ, η and z are the same above and below p_c. Moreover, the scaling relation in equation (28) is in both cases satisfied, although it was demonstrated only for $p > p_c$. Hence, there are only three independent scaling exponents, $\nu_{\perp}$, $\nu_{||}$ and δ, while z and η can be determined using the scaling relations in equations (24) and (28). The correlation length exponents are identical to those of DP in an infinite lattice while δ depends on the boundary conditions and, therefore, changes the universality class.

5. Summary and conclusions

We have obtained, through a MF analysis, the phase diagram of the stochastic sandpile model. There is a critical probability p_c above which the system is in a SOC state, where

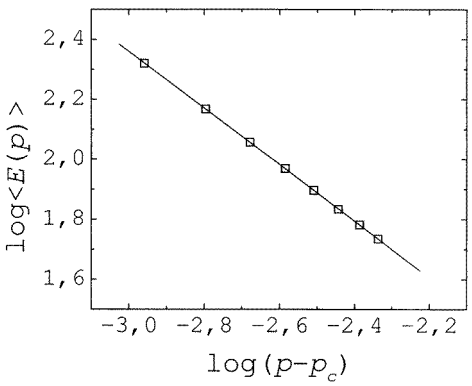

Figure 7. Average energy per lattice site as a function of p in the SOC state. The continuous line is a linear fit in the log–log scale.

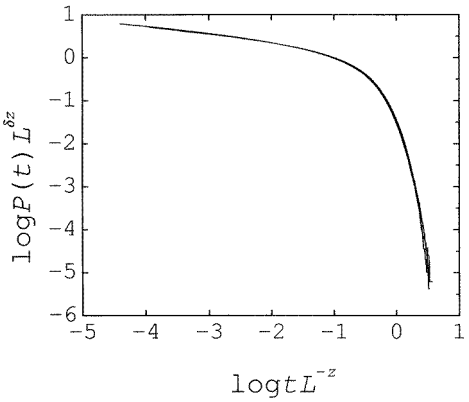

Figure 8. Data collapse plot for $P(t)$ in the SOC state for $L = 160$, 320 and 640.

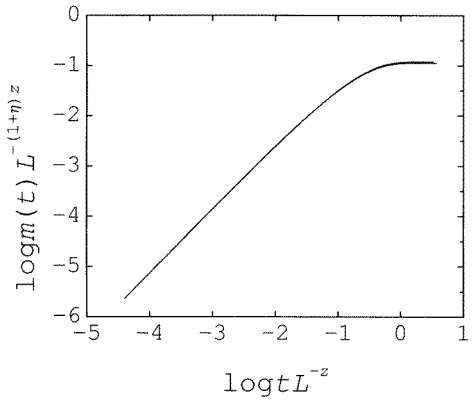

Figure 9. Data collapse plot for $m(t)$ in the SOC state for $L = 160$, 320 and 640.

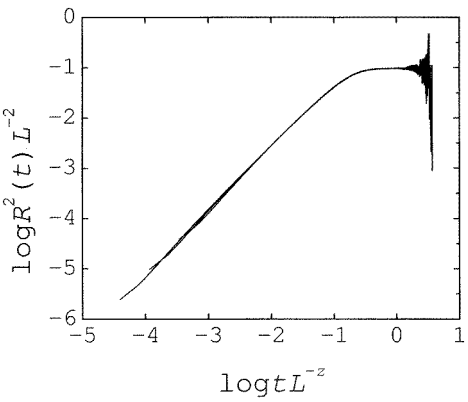

Figure 10. Data collapse plot for $R^2(t)$ in the SOC state for $L = 160$, 320 and 640.

the correlation lengths diverge in the thermodynamic limit. Below p_c the system is subcritical, it is characterized by a finite susceptibility which diverges when the critical state is approached. While the stationary state in the SOC state is characterized by a well-defined average energy per lattice site, the subcritical state is not completely stationary, since the average energy per lattice size increases linearly with time. Then, it has been shown that global conservation is a necessary condition to obtain SOC in sandpile models.

Using scaling arguments in the subcritical region, the analysis has shown that the stochastic sandpile model is similar to DP, but with different boundary conditions. On the other hand, the scaling theory in the SOC state reveals that global conservation introduces a constraint among the scaling exponents, generalizing previous results obtained for particular sandpile models. We have provided a general demonstration of the scaling law $\langle s \rangle \sim L^2$.

Numerical simulations validate the predictions of the MF and scaling theory. The correlation length exponents and the critical probability have been found, within the numerical error, to be identical to the estimates for DP. However, the existence of different boundary conditions and conservation law leads to differences in other exponents, changing the

universality class.

We must emphasize that the stochastic sandpile model is not just another cellular automaton showing SOC, but a very nice example with which to understand the differences and similarities between SOC and ordinary nonequilibrium critical phenomena. The comparison of the phase diagram of this model with that of DP reveals the essential property of SOC, the insensitivity to changes in model parameters. While the critical state in DP is restricted to a point in the phase diagram, in the stochastic sandpile model it is extended through a line segment.

Acknowledgments

This work was partially supported by the Alma Mater prize, given by The University of Havana, and the Ministerio de Educación y Cultura, Spain. This work was performed during the sabbatical leave of OS in the Departamento de Física, Matemática y Fluidos, UNED. We thank Alessandro Vespignani for helpful comments and discussions during the preparation of this manuscript, and J Castillo for his help in the redaction. The numerical simulations were performed using the computer resources of The Abdus Salam ICTP, during the visit of A Vázquez to this Centre under the 1998 Federation Arrangement.

References

[1] Bak P, Tang C and Wiesenfeld K 1987 *Phys. Rev. Lett.* **59** 381
[2] Tang C and Bak P 1988 *Phys. Rev. Lett.* **60** 2347
Tang C and Bak P 1988 *J. Stat. Phys.* **51** 797
[3] Vespignani A and Zapperi S 1997 *Phys. Rev. Lett.* **78** 4793
Vespignani A and Zapperi S 1998 *Phys. Rev.* E **57** 6345
[4] Grassberger P 1995 *J. Stat. Phys.* **79** 12 and references therein
[5] Janssen H K 1981 *Z. Phys.* B **42** 151
[6] Grassberger P 1982 *Z. Phys.* B **47** 365
[7] Olami Z, Procaccia I and Zeitak R 1994 *Phys. Rev.* E **49** 1232
[8] Grassberger P 1995 *Phys. Lett.* A **200** 277
[9] Tadić B and Dhar D 1997 *Phys. Rev. Lett.* **79** 1519
[10] Maslov S and Zhang Y-C 1996 *Physica* A **223** 1
[11] Manna S S 1991 *Physica* A **179** 249
[12] Caldarelli G 1997 *Physica* A **252** 295
[13] Essam J W, Guttmann A J, Jensen I and Tanlakishani D 1996 *J. Phys. A: Math. Gen.* **29** 1619
[14] Grassberger P and de la Torre A 1979 *Ann. Phys.* **122** 373
[15] Jensen I 1996 *J. Phys. A: Math. Gen.* **29** 7013
[16] Dhar D 1990 *Phys. Rev. Lett.* **64** 1613